Variational generalized Kohn-Sham approach combining the random-phase-approximation and Green's-function methods

Vamsee K. Voora, Sree Ganesh Balasubramani, and Filipp Furche

Phys. Rev. A **99**, 012518 — Published 28 January 2019

DOI: 10.1103/PhysRevA.99.012518

Variational Generalized Kohn–Sham Approach Combining Random Phase Approximation and Green's Function Methods

Vamsee K. Voora, Sree Ganesh Balasubramani, and Filipp Furche*
University of California, Irvine, Department of Chemistry, 1102 Natural Sciences II, Irvine, CA 92697-4095, USA

A generalized Kohn–Sham (GKS) scheme which variationally minimizes the random phase approximation (RPA) ground state energy with respect to the GKS one-particle density matrix is introduced. We introduce the notion of functional-selfconsistent (FSC) schemes, which vary the one-particle Kohn–Sham (KS) potential entering an explicitly potential-dependent exchange-correlation (XC) energy functional for a given density, and distinguish them from orbital-selfconsistent (OSC) schemes, which vary the density, or the orbitals, density matrix, or KS potential generating the density. It is shown that, for explicitly potential-dependent XC functionals, existing OSC schemes such as the optimized effective potential method violate the Hellmann-Feynman theorem for the density, producing a spurious discrepancy between the KS density and the correct Hellmann-Feynman density for approximate functionals. A functional selfconsistency condition is derived which resolves this discrepancy by requiring the XC energy to be stationary with respect to the KS potential at fixed density. We approximately impose functional selfconsistency by by semicanonical projection (sp) of the PBE KS Hamiltonian. Variational OSC minimization of the resulting GKS-spRPA energy functional leads to a nonlocal correlation potential whose off-diagonal blocks correspond to orbital rotation gradients, while its diagonal blocks are related to the RPA self-energy at real frequency. Quasiparticle *GW* energies are a first-order perturbative limit of the GKS-spRPA orbital energies; the lowest-order change of the total energy captures the renormalized singles excitation correction to RPA. GKS-spRPA orbital energies are found to approximate ionization potentials and fundamental gaps of atoms and molecules more accurately than semilocal density functional approximations (SL DFAs) or G_0W_0 and correct the spurious behavior of SL DFAs for negative ions. GKS-spRPA energy differences are uniformly more accurate than the SL-RPA ones; improvements are modest for covalent bonds but substantial for weakly bound systems. GKS-spRPA energy minimization also removes the spurious maximum in the SL-RPA potential energy curve of Be_2, and produces a single Coulson–Fischer point at ~ 2.7 times the equilibrium bond length in H_2. GKS-spRPA thus corrects most density-driven errors of SL-RPA, enhances the accuracy of RPA energy differences for electron-pair conserving processes, and provides an intuitive one-electron GKS picture yielding ionization potentials energies and gaps of *GW* quality.

I. INTRODUCTION AND SUMMARY

Electronic structure methods based on the random-phase approximation (RPA) [1, 2] are rapidly gaining popularity in solid-state and molecular applications [3–5]. As opposed to semilocal (SL) density functional approximations (DFAs), RPA-based methods capture noncovalent interactions [6], which have recently moved into the focus of research in soft matter, nanomaterials, and catalysis [7]. RPA-based methods are comparable in cost with but more robust than perturbative approaches for small-gap systems and offer a way out of the functional inflation dilemma faced by SL DFAs [8].

The vast majority of today's RPA calculations are performed in a "post Kohn–Sham" fashion, i.e., by evaluating the RPA energy functional using Kohn–Sham (KS) orbitals generated from a variational SL DFA calculation [9]. Apart from the lack of a variationally stable energy, a major limitation of this SL-RPA approach is that SL densities are relatively inaccurate for open-shell systems, negative ions, and small-gap compounds, producing large "density-driven errors" in energies and other properties [10, 11]. For example, SL DFAs produce qualitatively incorrect densities and ionization potentials for negative ions [12], and overly delocalized states for correlated materials [13].

Unlike SL energy functionals, the RPA energy explicitly depends on the unknown KS potential, making straightforward minimization with respect to the density or KS orbitals impossible. In this paper, we distinguish density- or orbital-selfconsistent (OSC) RPA approaches, which minimize the energy after choosing an approximate KS potential, from functional selfconsistent (FSC) approaches, which aim to determine the KS potential functional self-consistently by requiring its exchange-correlation (XC) part to coincide with the functional derivative of the RPA energy. The optimized effective potential (OEP) approach [14–17] has been claimed to achieve "fully selfconsistent" RPA results [16]. However, while OEP-RPA produces accurate KS orbital energies, OEP-RPA results for bond energies and noncovalent interactions are less accurate than their SL-RPA counterparts [16]. This result is puzzling, because the OEP-RPA KS potentials are considerably more accurate than SL ones [18], and recent orbital-optimized RPA approaches improve upon SL RPA energetics [19].

* Author to whom correspondence should be addressed. Email: filipp.furche@uci.edu

Observables such as quasiparticle spectra and ionization potentials (IPs) have traditionally been the domain of many-body Green's function theory (GFT) [20–22]. For example, quasiparticle self-consistent *GW* theory [23, 24] yields highly accurate IPs and band gaps for a wide variety of materials, but accurate total energy differences and related properties such as structures or thermodynamic quantities remain elusive. *GW* approaches starting from SL DFAs [25–27] and even fully self-consistent *GW* [28] face a similar dilemma, producing high quality quasiparticle spectra and excitation energies, but energy differences generally inferior to SL-RPA [29, 30].

Here we generalize the SL-RPA energy functional using a simple semicanonical projection (sp) of the SL KS Hamiltonian. The resulting spRPA energy is a functional of the KS one-particle density matrix that may variationally be minimized using an OSC generalized KS (GKS) scheme [31]. Semicanonical approaches have successfully been used to devise perturbative corrections to SL-RPA in the past [32]. The present variational GKS spRPA method is designed to (i) recover SL-RPA for SL densities; (ii) reduce density-driven error by determining the density from the stationary point of the RPA rather than a SL energy functional; (iii) systematically improve SL-RPA energetics; (iv) approximate FSC RPA without sacrificing the variational principle; (v) yield a complete GKS effective one-particle Hamiltonian, unlike orbital optimized [19] or Brueckner [33] RPA, providing an intuitive one-electron picture and GKS orbital energies which accurately approximate quasiparticle spectra [34]; (vi) establish a straightforward connection to GFT and *GW* theory; (vii) eliminate the need for KS inversion or OEP approaches, which can be ill conditioned [35] and require cumbersome regularization [36–38].

II. VARIATIONAL MINIMIZATION OF POTENTIAL-DEPENDENT FUNCTIONALS

A. Statement of the Problem

Variational minimization of a functional with respect to the density or the KS orbitals requires knowledge at least of the energy functional and its functional derivative for a given trial density. Here we consider functionals that depend on the density $\rho(x)$ through the KS orbitals and occupation numbers $|\phi_p\rangle$ and n_p *and explicitly* on the KS potential $\mathrm{V}_s[\rho](x)$; $x = (\mathbf{r}, \sigma)$ denotes space-spin coordinates. This large class includes functionals derived from many-body perturbation theory [39–41] as well as RPA. The resulting XC energy thus takes the general form

$$E^{\mathrm{XC}}[\rho] = E^{\mathrm{XC}}[|\boldsymbol{\phi}[\rho]\rangle, \mathbf{n}[\rho], \mathrm{V}_s[\rho]], \tag{1}$$

where the KS orbitals and occupation numbers were gathered in the column vectors $|\boldsymbol{\phi}\rangle, \mathbf{n}$.

Kohn and Sham[42] showed that variational minimization of the total energy as a functional of ρ leads to the KS equations

$$\mathrm{H}_0[\rho]\,|\phi_p\rangle = \epsilon_p\,|\phi_p\rangle\,, \tag{2}$$

where $\mathrm{H}_0[\rho] = \mathrm{T} + \mathrm{V}_s[\rho]$ is the noninteracting KS one-particle Hamiltonian, T is the one-particle kinetic energy operator, and

$$\mathrm{V}_s[\rho](x) = \mathrm{V}^{\mathrm{ext}}(x) + \mathrm{V}^{\mathrm{H}}[\rho](x) + \mathrm{V}^{\mathrm{XC}}[\rho](x) \tag{3}$$

is the KS one-particle potential. $\mathrm{V}^{\mathrm{ext}}(x)$ is the external one-particle potential, and $\mathrm{V}^{\mathrm{H}}[\rho](x)$ is the Hartree potential. The XC potential is the (total) functional derivative of the XC energy with respect to the density,

$$\mathrm{V}^{\mathrm{XC}}[\rho](x) = \frac{\delta E^{\mathrm{XC}}[\rho]}{\delta\rho(x)}. \tag{4}$$

The OSC minimizing density is given by

$$\rho(x) = \sum_p n_p |\phi_p(x)|^2, \tag{5}$$

with occupation numbers normally [43] chosen according to the Aufbau principle. While this section focuses on density-based "proper KS" schemes, analogous considerations apply to the GKS framework [31], if the local XC potential in Eq. (4) is replaced by the nonlocal one defined by the functional derivative of the XC energy with respect to the KS density matrix.

However, Eqs. (1)-(5) do not completely determine the energy as a functional of the density: Obtaining the KS potential via Eq. (4) requires knowledge of $E^{\mathrm{XC}}[\rho]$, which in turn is defined in terms of the KS potential. Two different avenues have been used to bypass this quandary: The first uses the density (or, in GKS framework, the orbitals and occupation numbers) as independent variable. In this case, an additional condition specifying the KS potential as a functional of the density (or the orbitals and occupation numbers) is required. The second approach considers the density (or the orbitals and occupation numbers) as dependent variable(s), and the potential as independent variable. This potential-functional approach requires specification of the density (or the orbitals and occupation numbers) as functional of the potential. In the following, we discuss different choices for either functional(s), which lead to qualitatively different XC energy functionals, labeled by subscripts *a*-*d*.

B. KS Potentials and Energy Functionals

a. Semilocal Potentials. Since SL KS potentials are readily available, a straightforward choice for the XC energy functional is

$$E_a^{\mathrm{XC}}[\rho] = E^{\mathrm{XC}}[|\boldsymbol{\phi}[\rho]\rangle, \mathbf{n}[\rho], \mathrm{V}_s^{\mathrm{SL}}[\rho]]. \tag{6}$$

Here, the SL XC potential is the functional derivative of a SL XC energy functional such as PBE [44],

$$\mathrm{V}^{\mathrm{XC\ SL}}[\rho](x) = \frac{\delta E^{\mathrm{XC\ SL}}[\rho]}{\delta\rho(x)}, \tag{7}$$

and $\mathrm{V}_s^{\mathrm{SL}}[\rho]$ is obtained by replacing $\mathrm{V}^{\mathrm{XC}}[\rho]$ with $\mathrm{V}^{\mathrm{XC\ SL}}[\rho]$ in Eq. (3).

The main drawback of this approach is that it violates Eq. (4),

$$\frac{\delta E_a^{\mathrm{XC}}[\rho]}{\delta\rho(x)} \neq \mathrm{V}^{\mathrm{XC\ SL}}[\rho](x). \tag{8}$$

As a result, there are two KS systems, one related to minimization of $E_a^{\mathrm{XC}}[\rho]$, and the other generated by $\mathrm{V}^{\mathrm{XC\ SL}}[\rho]$, whose density is generally different from the orbital density ρ. The XC energy is defined in terms of the relatively inaccurate SL potential, giving rise to density-driven error. In explorative calculations using the RPA energy functional, the total energy differences we obtained from such schemes were not significantly more accurate than the post-KS semilocal ones.

b. "Exact" Potentials Via KS Inversion or OEP. For a noninteracting v-representable trial density, the "exact" KS potential $\mathrm{V}_s[\rho]$ (and thus $\mathrm{H}_0[\rho]$) may be determined, up to a constant, by inversion of the KS equations. One thus might wonder if this choice results in better properties than the use of SL potentials. While the uniqueness of $\mathrm{V}_s[\rho]$ is guaranteed by the Hohenberg–Kohn theorem [45], general trial densities may not be pure-state noninteracting v-representable; see, e.g., Ref. 46 for examples. In common finite basis sets, this condition is rarely satisfied [47], and KS inversion procedures can be ill-posed [48].

The OEP approach claims to bypass some of these difficulties [14–16, 40] by using the local KS potential $\mathrm{V}_s(x)$ as independent variable[49, 50] and the KS orbitals $\phi_p[\mathrm{V}_s]$ and occupation numbers $n_p[\mathrm{V}_s]$ as dependent variables; the functionals $\phi_p[\mathrm{V}_s]$ and $n_p[\mathrm{V}_s]$ are defined by the requirement that they satisfy the KS equations (2) and minimize the total KS kinetic energy. The resulting XC energy thus becomes a potential functional,

$$E_b^{\mathrm{XC}}[\mathrm{V}_s] = E_b^{\mathrm{XC}}[|\boldsymbol{\phi}[\mathrm{V}_s]\rangle, \mathbf{n}[\mathrm{V}_s], \mathrm{V}_s]. \tag{9}$$

To make a connection to density functionals, OEP methods consider the density generated by the KS orbitals and occupation numbers,

$$\rho_s[\mathrm{V}_s](x) = \sum_p n_p[\mathrm{V}_s]|\phi_p[\mathrm{V}_s](x)|^2. \tag{10}$$

By the HK theorem, V_s is a functional of ρ_s, and thus the XC potential can be obtained from the chain rule,

$$\frac{\delta E_b^{\mathrm{XC}}[\mathrm{V}_s]}{\delta \mathrm{V}_s(x)} = \int dx' \frac{\delta E_b^{\mathrm{XC}}[\rho_s]}{\delta\rho_s(x')} \frac{\delta\rho_s[\mathrm{V}_s](x')}{\delta \mathrm{V}_s(x)}. \tag{11}$$

Since $\rho_s[\mathrm{V}_s]$ is the KS density, $\delta\rho_s[\mathrm{V}_s](x')/\delta \mathrm{V}_s(x)$ is the well-known KS density-density response function, which is an explicit functional of the KS orbitals and orbital energies for a given potential V_s [16, 40], and Eq. (11) becomes the OEP integral equation [51]. While grid-based OEP approaches are fairly straightforward, basis-set OEP approaches can be ill-posed similar to KS inversion [35] and require additional regularization [36–38].

OEP approaches to potential-dependent XC functionals have been dubbed "fully selfconsistent" [16, 52]. Even though they use the "exact" KS potential, however, they lack functional selfconsistency, causing the KS density ρ_s to differ from the functional derivative of the energy with respect to the external potential:

In potential functional theory, the density as a functional of the KS potential is *defined* by

$$\frac{\delta E[\mathrm{V}_s]}{\delta \mathrm{V}^{\mathrm{ext}}(x)} = \rho[\mathrm{V}_s](x), \tag{12}$$

where $E[\mathrm{V}_s]$ is the total energy potential functional [49, 53]. Eq. (12) is the equivalent of Eq. (4) in density functional theory and thus fundamental; it may be viewed a consequence of the Hellmann-Feynman theorem, and as such is commonly used to define the density and all related properties even for approximate energy functionals. For inexact XC functionals with explicit dependence on the KS potential, however, the KS density, defined by Eq. (10), generally differs from the exact one, defined by Eq. (12): Evaluating the functional derivative of the total energy expression defined by the potential functional $E_b^{\mathrm{XC}}[\mathrm{V}_s]$ in Eq. (9) using the Hellmann-Feynman theorem and Eq. (12) yields

$$\rho_s[\mathrm{V}_s] + \left(\frac{\delta E_b^{\mathrm{XC}}[\mathrm{V}_s]}{\delta \mathrm{V}_s(x)}\right)_{|\boldsymbol{\phi}[\mathrm{V}_s]\rangle, \mathbf{n}[\mathrm{V}_s]} = \rho_b[\mathrm{V}_s](x), \tag{13}$$

where the functional derivative is a partial derivative at fixed orbitals and occupation numbers, and $\rho_b[\mathrm{V}_s](x) = \delta E_b[\mathrm{V}_s]/\delta \mathrm{V}^{\mathrm{ext}}(x)$ is the Hellmann-Feynman density generated by $E_b^{\mathrm{XC}}[\mathrm{V}_s]$. The quantity

$$\rho_b^{\mathrm{XC}}[\mathrm{V}_s](x) = \left(\frac{\delta E_b^{\mathrm{XC}}[\mathrm{V}_s]}{\delta \mathrm{V}_s(x)}\right)_{|\boldsymbol{\phi}[\mathrm{V}_s]\rangle, \mathbf{n}[\mathrm{V}_s]}, \tag{14}$$

is zero for the exact XC functional by construction, but generally nonzero for the approximate explicitly potential-dependent XC functionals discussed here (see, e.g., Ref. 16 and Sec. III B for examples). An immediate consequence is that

$$\frac{\delta E_b^{\mathrm{XC}}[\rho_s]}{\delta\rho_s(x)} \neq \frac{\delta E_b^{\mathrm{XC}}[\rho_b]}{\delta\rho_b(x)}, \tag{15}$$

i.e., the OEP XC potential produces the functional derivative of the XC energy with respect to the noninteracting KS density ρ_s rather than $\rho_b[\mathrm{V}_s]$, which is the correct density by Eq. (12).

In conclusion, even using the "exact" KS potential produces the paradoxical result of two different densities corresponding to two different KS potentials, and the less accurate of the two (according to the Hellmann-Feynman

theorem) is used to obtain the total energy. This confirms that lacking functional selfconsistency is a fundamental problem of explicitly potential-dependent functionals which, contrary to previous suggestions [16, 40], cannot be remedied by the OEP approach.

c. Functional-Selfconsistent Potentials. The paradoxical result of two different densities and KS potentials are caused by inconsistency of the KS potentials defining the XC energy functional with the functional derivative thereof. A resolution is possible if the KS potential satisfies the functional selfconsistency condition

$$\rho^{\mathrm{XC}}[|\boldsymbol{\phi}\rangle, \mathbf{n}, \mathrm{V}_s](x) = 0. \tag{16}$$

By Eq. (13), the orbitals and occupation numbers generated by such an FSC KS potential yield the correct Hellmann-Feynman density, and thus Eq. (16) is an exact constraint for the KS potential V_s. Eq. (16) is equivalent to requiring the XC energy functional to be stable with respect to variations of the KS potential at fixed orbitals and occupation numbers. Thus, the chain rule yields for the FSC XC potential

$$\begin{aligned} \mathrm{V}^{\mathrm{XC}}[|\boldsymbol{\phi}\rangle, \mathbf{n}, \mathrm{V}_s](x) &= \frac{\delta E^{\mathrm{XC}}[|\boldsymbol{\phi}\rangle, \mathbf{n}, \mathrm{V}_s]}{\delta\rho(x)} \\ &= \left(\frac{\delta E^{\mathrm{XC}}[|\boldsymbol{\phi}\rangle, \mathbf{n}, \mathrm{V}_s]}{\delta\rho(x)}\right)_{\mathrm{V}_s}, \end{aligned} \tag{17}$$

since the partial derivative with respect to V_s vanishes according to Eq. (16). For potential-independent XC functionals, the partial derivative is a total derivative, and Eq. (17) reduces to the conventional definition of the XC potential. For potential-dependent XC functionals, Eq. (17) is a statement of the functional selfconsistency condition.

It may be possible to define a FSC XC potential $\mathrm{V}_{s,c}[|\boldsymbol{\phi}\rangle, \mathbf{n}]$ as a functional of the orbitals and occupation numbers implicitly by Eqs. (16) or (17). The conditions under which the functional selfconsistency constraint uniquely determines $\mathrm{V}_{s,c}$ and the resulting XC energy functional

$$E_c^{\mathrm{XC}}[|\boldsymbol{\phi}\rangle, \mathbf{n}] = E^{\mathrm{XC}}[|\boldsymbol{\phi}\rangle, \mathbf{n}, \mathrm{V}_{s,c}[|\boldsymbol{\phi}\rangle, \mathbf{n}]] \tag{18}$$

depend on the specific form of the XC energy functional (1). If such a unique potential $\mathrm{V}_{s,c}$ exists, then the density (or KS orbitals and occupation numbers) minimizing the energy functional associated with E_c^{XC} are generated by it, because, by Eq. (17), $\mathrm{V}_{s,c}$ is obtained from the functional derivative of E_c^{XC}. At the same time, Eq. (16) guarantees that the resulting KS density equals the Hellman-Feynman one. In this sense, the FSC KS potential is optimal for a given explicitly potential-dependent energy functional.

It is important to distinguish orbital and functional selfconsistency in such a scheme: The latter determines the KS potential and thus the energy functional for *fixed* density, while the former determines the minimizing density (or the KS orbitals and occupation numbers). Mixing the two may produce ill-defined energy functionals, causing problems such as initial state dependence and multiple solutions familiar from selfconsistent GFT approaches [54].

d. Semicanonical KS. The above analysis suggests that lack of functional selfconsistency of SL and OEP KS potentials critically limits the accuracy of these approaches. We take a step towards a fully FSC solution by constructing an approximation to the FSC KS Hamiltonian, which leads to an explicit energy functional of the orbitals and occupation numbers. Using a GKS framework to achieve orbital selfconsistency allows us to bypass the numerical challenges of OEP methods and obtain orbital energies corresponding to physical ionization potentials and electron affinities.

Rather than imposing the full functional selfconsistency condition, which implies that the KS potential entering the XC energy functional is identical to the functional derivative thereof, see Eq. (17), we only require that the KS potential defining the XC energy generate the same eigenstates (up to unitary equivalence) as the one obtained from functional differentiation. This weaker condition is readily imposed by semicanonical projection of a readily available SL KS Hamiltonian $\mathrm{H}_0^{\mathrm{SL}}$. In the most general case, the KS density matrix takes the form

$$\mathrm{D} = \sum_{\lambda\lambda'} \mathrm{P}_\lambda \mathrm{n}_{\lambda\lambda'} \mathrm{P}_{\lambda'}, \tag{19}$$

where P_λ denotes orthogonal projectors belonging to blocks of KS orbitals with degenerate occupation numbers, and $\mathrm{n}_{\lambda\lambda'} = \mathrm{n}_\lambda \delta_{\lambda\lambda'}$ is diagonal, with n_λ denoting occupation number matrices [55], see Appendix A. For example, for integer KS occupations $1, 0$, there are two distinct matrices n_λ with eigenvalues $n_\lambda = 1, 0$. The sp KS Hamiltonian is defined by

$$\tilde{\mathrm{H}}_0 = \sum_\lambda \mathrm{P}_\lambda \mathrm{H}_0^{\mathrm{SL}} \mathrm{P}_\lambda, \tag{20}$$

and contains only the diagonal ($\lambda = \lambda'$) blocks of $\mathrm{H}_0^{\mathrm{SL}}$. $\tilde{\mathrm{H}}_0$ commutes with D by construction; thus, one may find a common "semicanonical" basis in which both $\tilde{\mathrm{H}}_0$ and a given KS density matrix are diagonal. Moreover, $\tilde{\mathrm{H}}_0$ is invariant under unitary transformations of KS orbitals with degenerate occupation numbers, since the projectors P_λ are invariant. If D is generated by $\mathrm{H}_0^{\mathrm{SL}}$, then $\tilde{\mathrm{H}}_0 = \mathrm{H}_0^{\mathrm{SL}}$; perturbation theory implies that the deviation of the sp orbital energies from the SL ones is quadratic in $\mathrm{H}_0^{\mathrm{SL}} - \tilde{\mathrm{H}}_0$. The nonlocal sp XC potential may thus be defined as

$$\tilde{\mathrm{V}}^{\mathrm{XC}}[|\boldsymbol{\phi}\rangle, \mathbf{n}] = \mathrm{V}^{\mathrm{XC\ SL}}[\rho] + \tilde{\mathrm{H}}_0[|\boldsymbol{\phi}\rangle, \mathbf{n}] - \mathrm{H}_0^{\mathrm{SL}}[\rho], \tag{21}$$

and the corresponding sp XC energy functional,

$$E_d^{\mathrm{XC}}[|\boldsymbol{\phi}\rangle, \mathbf{n}] = E^{\mathrm{XC}}[|\boldsymbol{\phi}\rangle, \mathbf{n}, \tilde{\mathrm{V}}^{\mathrm{XC}}[[|\boldsymbol{\phi}\rangle, \mathbf{n}]], \tag{22}$$

is an explicit functional of the KS orbitals and occupation numbers only, which may be subject to OSC optimization using GKS methodology. We will thus focus on functional of type $E_d^{\mathrm{XC}}[|\boldsymbol{\phi}\rangle, \mathbf{n}]$ in the following.

C. spRPA Energy Functional

For a given KS determinant Φ, the RPA total energy,

$$E^{\mathrm{RPA}} = \langle\Phi|\mathrm{H}|\Phi\rangle + E^{\mathrm{C\ RPA}}, \tag{23}$$

equals the expectation value of the physical Hamiltonian H plus the RPA correlation energy, [56, 57]

$$E^{\mathrm{C\ RPA}} = -\frac{1}{2}\int_0^1 d\alpha \Im \int_{-\infty}^{\infty} \frac{d\omega}{2\pi} \langle \left(\Pi_\alpha^{\mathrm{RPA}}(\omega) - \Pi_0(\omega)\right) \mathrm{V}\rangle. \tag{24}$$

V is the bare electron-electron Coulomb interaction, $\Pi_\alpha^{\mathrm{RPA}}(\omega) = (1-\alpha\Pi_0(\omega)\mathrm{V})^{-1}\Pi_0(\omega)$ denotes the time-ordered RPA polarization propagator at coupling strength α and real frequency ω, and $\Pi_0(\omega)$ is its noninteracting KS equivalent; brackets stand for traces. The rank four operator $\Pi_0(\omega)$ factorizes as [58]

$$\Pi_0(\omega) = \int_{-\infty}^{\infty} \frac{d\omega'}{2\pi i} \mathrm{G}_0(\omega') \otimes \mathrm{G}_0(\omega' - \omega), \tag{25}$$

into a convolution product of one-particle KS Green's functions $\mathrm{G}_0(\omega)$.

The KS Green's function corresponding to the sp KS Hamiltonian $\tilde{\mathrm{H}}_0$ is

$$\begin{aligned}\mathrm{G}_0(\omega) = {} & \mathrm{n}^{1/2}(\omega - \tilde{\mathrm{H}}_0 - i0^+)^{-1}\mathrm{n}^{1/2} \\ & + (1-\mathrm{n})^{1/2}(\omega - \tilde{\mathrm{H}}_0 + i0^+)^{-1}(1-\mathrm{n})^{1/2};\end{aligned} \tag{26}$$

this symmetrized form remains Hermitian even for density matrix variations causing off-diagonal occupation number matrices. By construction, $\mathrm{G}_0(\omega)$ reproduces D,

$$\mathrm{D} = \int_{-\infty}^{\infty} \frac{d\omega}{2\pi i} e^{i\omega 0^+} \mathrm{G}_0(\omega). \tag{27}$$

On the other hand, the quasiparticle spectrum of the sp Green's function is given by the semicanonical KS eigenvalues of $\tilde{\mathrm{H}}_0$, which approximate the semilocal ones in a perturbative sense.

Eqs. (20)-(26) define the spRPA energy as a functional of the KS density matrix, $E^{\mathrm{spRPA}}[\mathrm{D}]$, or, equivalently, the spectral projectors P_λ and occupation number matrices n_λ – clearly, a functional of type d according to Sec. II B. $E^{\mathrm{spRPA}}[\mathrm{D}]$ depends on the SL XC potential DFA entering $\tilde{\mathrm{H}}_0$, for which we choose PBE [44]. This introduces a dependence on the choice of SL potential; however, this dependence is less strong than for SL-RPA, see Section IV of the Supplemental Material (SM) [59], since the current scheme is OSC and partially FSC, and even for SL-RPA, the dependence of energy difference on the specific choice of SL potential is moderate [3]. The spRPA energy functional is conveniently evaluated by expressing G_0 in the semicanonical basis, factorizing the interaction V, and performing the frequency integration along the imaginary axis, in analogy to SL-RPA [60].

III. VARIATIONAL GKS MINIMIZATION OF SEMICANONICAL PROJECTED RPA

A. Energy Lagrangian and Euler Equations

Within the GKS-spRPA formalism, the ground state energy is obtained as the minimum of the spRPA energy functional with respect to D, subject to the Fermion N-representability constraint that D have eigenvalues between 0 and 1 whose sum is the total electron number N. We explicitly impose the latter by the substitution $\mathrm{n} = \mathrm{m}^\dagger\mathrm{m}$, where the Hermitian matrices m satisfy $\langle \mathrm{m}^\dagger\mathrm{m}\rangle = N$. The GKS-spRPA energy Lagrangian is thus

$$\begin{aligned}L^{\mathrm{spRPA}}[|\boldsymbol{\phi}\rangle, \mathrm{m}, \eta, \mu] = {} & E^{\mathrm{spRPA}}[\mathrm{D}[|\boldsymbol{\phi}\rangle, \mathrm{m}]] \\ & - \langle \eta(\langle\boldsymbol{\phi}|\boldsymbol{\phi}\rangle - 1)\rangle - \mu\left(\langle \mathrm{m}^\dagger\mathrm{m}\rangle - N\right).\end{aligned} \tag{28}$$

Here, the GKS orbitals were gathered in the transpose vectors $|\boldsymbol{\phi}\rangle$, i.e., $\langle\boldsymbol{\phi}|\boldsymbol{\phi}\rangle$ is a matrix with respect to GKS orbital indices (but a scalar with respect to the one-particle Hilbert space). In this notation, the GKS density matrix becomes

$$\mathrm{D}[|\boldsymbol{\phi}\rangle, \mathrm{m}] = |\boldsymbol{\phi}\rangle\, \mathrm{m}^\dagger\mathrm{m}\, \langle\boldsymbol{\phi}|. \tag{29}$$

the Hermitian Lagrange multiplier matrix η enforces orbital orthonormality, and the real scalar Lagrange multiplier μ accounts for normalization of D. The present approach is a special case of variational density matrix functional minimization [55, 61, 62]. A necessary condition for a minimum of the GKS-spRPA energy subject to the above constraints is that the first partial derivatives of L^{spRPA} with respect to all variational parameters vanish.

Requiring stationarity with respect to the GKS orbitals leads to the GKS self-consistent field (SCF) equations

$$\mathrm{H}_0^{\mathrm{spRPA}}[\mathrm{D}]\, \mathrm{n}\, |\boldsymbol{\phi}\rangle = \eta\, |\boldsymbol{\phi}\rangle, \tag{30}$$

where the effective one-particle GKS-spRPA Hamiltonian is defined as the functional derivative of the spRPA energy with respect to the GKS density matrix,

$$\mathrm{H}_0^{\mathrm{spRPA}}[\mathrm{D}] = \frac{\delta E^{\mathrm{spRPA}}[\mathrm{D}]}{\delta \mathrm{D}}. \tag{31}$$

Eq. (30) is equivalent to

$$\mathrm{H}_0^{\mathrm{spRPA}}\mathrm{n} = \eta. \tag{32}$$

The Hermiticity of all three matrices in the previous equation then implies that $\mathrm{H}_0^{\mathrm{spRPA}}$ and n commute, and since n is block-diagonal, so must be $\mathrm{H}_0^{\mathrm{spRPA}}$, i.e., matrix elements of the spRPA Hamiltonian between orbitals belonging to different occupation number blocks must vanish ("Brillouin's Theorem"). Evaluating n_λ as $\mathrm{n}_{ij\lambda} = n_\lambda \delta_{ij}$, where indices i, j label orbitals with identical occupation numbers n_λ, and defining the Hermitian

matrices

$$\epsilon_{\lambda\lambda'} = \begin{cases} 0 & \lambda \neq \lambda', \\ \eta_{\lambda\lambda}/n_\lambda & \lambda = \lambda', \end{cases} \tag{33}$$

Eq. (30) takes a more familiar form,

$$\mathrm{H}_0^{\mathrm{spRPA}}[\mathrm{D}]\,|\phi_{i\lambda}\rangle = \sum_j \epsilon_{ij\lambda}\,|\phi_{j\lambda}\rangle\,. \tag{34}$$

Eq. (34) is form-invariant under unitary transformations of orbitals belonging to degenerate occupation numbers n_λ. A unique "canonical" GKS-spRPA orbital basis may be defined by requiring $\epsilon_{ij\lambda}$ to be diagonal with elements $\epsilon_{i\lambda}$, in which case takes the form of the canonical GKS equations,

$$\mathrm{H}_0^{\mathrm{spRPA}}[\mathrm{D}]\,|\phi_{i\lambda}\rangle = \epsilon_{i\lambda}\,|\phi_{i\lambda}\rangle\,, \tag{35}$$

which need to be solved iteratively along with the orthonormality and normalization constraints.

The occupation numbers are determined by the stationarity condition for m,

$$(\mathrm{H}_0^{\mathrm{spRPA}} - \mu)\mathrm{m} = 0. \tag{36}$$

In the canonical basis, Eq. (36) simplifies to $(\epsilon_{i\lambda} - \mu)n_\lambda^{1/2} = 0$. The second variation of L^{spRPA} with respect to m is nonnegative for bound states with an Aufbau occupation, i.e., for all i,

$$n_\lambda = \begin{cases} 1; & \epsilon_{i\lambda} < \mu \\ 0; & \epsilon_{i\lambda} > \mu \end{cases}, \tag{37}$$

where the ionization potential μ is chosen such that the normalization condition $\langle \mathrm{n} \rangle = N$ is satisfied. If $\epsilon_{i\lambda} = \mu$, then any n_λ with $0 \leq n_\lambda \leq 1$ yielding correct normalization is permissible[55].

B. One-Particle GKS-spRPA Hamiltonian

The effective one-particle GKS-spRPA Hamiltonian may be analyzed by decomposing the functional derivative in Eq. (31) according to

$$\mathrm{H}_0^{\mathrm{spRPA}}[\mathrm{D}] = \mathrm{H}_0^{\mathrm{HF}}[\mathrm{D}] + \mathrm{V}^{\mathrm{C\ spRPA}}[\mathrm{D}]. \tag{38}$$

Here, $\mathrm{H}_0^{\mathrm{HF}}[\mathrm{D}]$ is the well-known Hartree-Fock one-particle Hamiltonian, and $\mathrm{V}^{\mathrm{C\ spRPA}}[\mathrm{D}]$ denotes the nonlocal RPA correlation potential resulting from the functional derivative of the spRPA correlation energy. Since the spRPA correlation energy depends on D only through the sp Green's function, Eq. (26), the functional chain rule yields

$$\mathrm{V}^{\mathrm{C\ spRPA}}[\mathrm{D}] = \int_{-\infty}^{\infty} \frac{d\omega}{2\pi} \Sigma^{\mathrm{C}}(\omega) \frac{\delta \mathrm{G}_0(\omega)}{\delta \mathrm{D}}. \tag{39}$$

The functional derivative $\delta \mathrm{G}_0(\omega)/\delta \mathrm{D}$ is a rank-four tensor operator whose properties are analyzed in Appendix B;

$$\Sigma^{\mathrm{C}}(\omega) = \frac{\delta E^{\mathrm{C\ spRPA}}}{\delta \mathrm{G}_0(\omega)} \tag{40}$$

is the correlation part of the RPA self-energy [18]. Eqs. (39) and (40) hold for any correlation energy functional of the GKS Green's function, and reveal the close connection of the GKS correlation potential and the corresponding self-energy. If the correlation energy further depends on G_0 through Π_0 only, then the functional chain rule may be used once more to show that the correlation self-energy has the form[20, 21]

$$\Sigma^{\mathrm{C}}(\omega) = \int_{-\infty}^{\infty} \frac{d\omega'}{\pi i} \mathrm{W}^{\mathrm{C}}(\omega')\mathrm{G}_0(\omega' - \omega). \tag{41}$$

The correlation part of the effective interaction

$$\mathrm{W}^{\mathrm{C}}(\omega) = \frac{\delta E^{\mathrm{C\ RPA}}}{\delta \Pi_0(\omega)} \tag{42}$$

is also a rank four tensor operator. Within RPA,

$$\mathrm{W}^{\mathrm{C}}(\omega) = \mathrm{V}(1 - \Pi_0(\omega)\mathrm{V})^{-1}; \tag{43}$$

thus, $\Sigma^{\mathrm{C}}(\omega)$ is identical to the correlation part of the GW self-energy [63, 64], evaluated at the spGKS Green's function.

To gain further insight into the physical meaning of the nonlocal RPA correlation potential, one may decompose the total density matrix derivative into a sum of three partial derivatives,

$$\mathrm{V}^{\mathrm{C\ spRPA}}[\mathrm{D}] = \mathrm{V}^{\mathrm{C},1}[\mathrm{D}] + \mathrm{V}^{\mathrm{C},2}[\mathrm{D}] + \mathrm{V}^{\mathrm{C},3}[\mathrm{D}]. \tag{44}$$

The first term corresponds to the partial density matrix derivative at fixed sp Hamiltonian $\tilde{\mathrm{H}}_0$. Using Appendix B and denoting (anti)commutators by (curly) brackets, this part of the potential is found to be

$$\mathrm{V}^{\mathrm{C},1}_{\lambda\lambda'} = \int \frac{d\omega}{2\pi} \begin{cases} \frac{1}{n_\lambda - n_{\lambda'}} \left[\mathrm{G}_0(\omega), \Sigma^{\mathrm{C}}(\omega)\right]_{\lambda\lambda'}, & \lambda \neq \lambda', \\ \pi i \left\{\delta(\omega - \tilde{\mathrm{H}}_0), \Sigma^{\mathrm{C}}(\omega)\right\}_{\lambda\lambda'}, & \lambda = \lambda'. \end{cases} \tag{45}$$

The off-diagonal ($\lambda \neq \lambda'$) blocks of $\mathrm{V}^{\mathrm{C},1}$ reduce to the gradient of the RPA energy with respect to orbital rotations, thus establishing a link to orbital-optimized RPA approaches [19]. The diagonal ($\lambda = \lambda'$) blocks, on the other hand, result from variations corresponding to changes in the occupation numbers and cannot be obtained in an orbital optimization framework. In the semicanonical basis, the λ blocks of $\tilde{\mathrm{H}}_0$ are diagonal,

$$\tilde{\mathrm{H}}_{0ij\lambda} = \delta_{ij}\tilde{\epsilon}_{i\lambda}, \tag{46}$$

and thus the diagonal blocks of $\mathrm{V}^{\mathrm{C},1\ \mathrm{spRPA}}$ take the form

$$\mathrm{V}^{\mathrm{C},1}_{ij\lambda} = \frac{i}{2}\left(\Sigma^{\mathrm{C}}_{\lambda ij}(\tilde{\epsilon}_{i\lambda}) + \Sigma^{\mathrm{C}}_{\lambda ji}(\tilde{\epsilon}_{j\lambda})\right). \tag{47}$$

Perturbative expansion of the GKS-spRPA orbital energies around the SL ground state solution reveals the physical significance of Eq. (47):

$$\epsilon_{i\lambda} = \epsilon^{\mathrm{SL}}_{i\lambda} + i\Sigma^{\mathrm{XC}}_{ii\lambda}(\epsilon^{\mathrm{SL}}_{i\lambda}) + V^{\mathrm{C},3}_{ii\lambda} - V^{\mathrm{XC\ SL}}_{ii\lambda} + O(\|\mathrm{H}_0^{\mathrm{spRPA}} - \mathrm{H}_0^{\mathrm{SL}}\|^2). \quad (48)$$

Here, $\Sigma^{\mathrm{XC}}(\omega)$ is the XC self-energy within the G_0W_0 approximation, and $V^{\mathrm{XC\ SL}}$ is the SL XC potential. The GKS-spRPA orbital energies hence reduce to the quasiparticle GW energies with unit normalization factor [21] in a perturbative first-order SCF sense apart from $\mathrm{V}^{\mathrm{C},3}$, which is typically small compared to $\mathrm{V}^{\mathrm{C},1}$.

The remaining parts of the GKS-spRPA correlation potential arise from changes in $\tilde{\mathrm{H}}_0$, see Appendix C. The second term accounts for the semicanonical projection and its diagonal part vanishes,

$$\mathrm{V}^{\mathrm{C},2}_{\lambda\lambda'} = \begin{cases} \frac{1}{n_\lambda - n_{\lambda'}}[\mathrm{H}_0^{\mathrm{SL}}, \mathrm{T}]_{\lambda\lambda'}, & \lambda \neq \lambda', \\ 0, & \lambda = \lambda', \end{cases} \quad (49)$$

Here, the RPA unrelaxed difference density matrix [65] or first-order density matrix [64]

$$\mathrm{T} = \frac{\delta E^{\mathrm{C\ spRPA}}}{\delta \tilde{\mathrm{H}}_0} \quad (50)$$

familiar from RPA analytical derivative theory has been introduced. Since the spGKS RPA Lagrangian is stationary at the converged spGKS density matrix D, there are no additional "orbital relaxation" terms, and the corresponding total interacting spRPA one-particle density matrix is simply D + T; an explicit expression for T is provided in Appendix C. The density generated by T equals $\rho^{\mathrm{XC}}(x)$, Eq. (14). Since GKS-spRPA is not fully FSC, $\rho^{\mathrm{XC}}(x)$ does not vanish, but is found to be small in most circumstances. The remaining part of the correlation potential,

$$\mathrm{V}^{\mathrm{C},3} = \mathrm{F}^{\mathrm{HXC}}\mathrm{T} \quad (51)$$

accounts for changes in the density entering the SL Hamiltonian due to $\rho^{\mathrm{XC}}(x)$; $\mathrm{F}^{\mathrm{HXC}}$ is the SL Hartree-, exchange-, and correlation (HXC) kernel.

IV. RESULTS

A. Ionization Potentials and Fundamental Gaps

Comparison of the computed highest occupied molecular orbital energies to the experimental first IPs of negatively charged atoms, see Table I, suggests that GKS-spRPA is substantially more accurate than G_0W_0 for negative ions, where G_0W_0 suffers from density-driven error. The GKS-spRPA highest occupied molecular orbital (HOMO) energies also improve greatly upon SL DFAs, and negative ions such as H^- are correctly bound.

TABLE I. Comparison of highest occupied molecular orbital (HOMO) energies (in eV) to experimental vertical ionization potentials for negatively charged atoms. G_0W_0 calculations were carried out using PBE orbitals. aug-cc-pVTZ basis sets [66, 67] were used.

	PBE	HF	G_0W_0	GKS-spRPA	Ref.
H^-	+1.5	−1.4	+0.3	−0.9	−0.75[a]
Li^-	+0.8	−0.4	−0.0	−0.8	−0.68[b]
F^-	+1.5	−4.9	−1.9	−3.2	−3.40[c]
Au^-	+0.5	−1.2	−1.7	−2.4	−2.31[d]

[a] Ref. [68]
[b] Ref. [69]
[c] Ref. [70]
[d] Ref. [71]

TABLE II. Mean absolute (MAE), mean signed (MSE, computed−reference) and maximum absolute (Max AE) errors (eV) for highest occupied molecular orbital energies of GW27 testset [27]. For reference values, negative of the ionization potentials from CCSD(T) were used [72]. def2-TZVPP basis-sets [73] was used for CCSD (T), PBE, HF, G_0W_0 and GKS-spRPA. For comparison, OEP-RPA results from Ref. [16] using aug-cc-pCVTZ basis-sets [74] are also shown. For G_0W_0 and GKS-spRPA, the exchange-correlation potential was approximated using the PBE functional.

Error Measure	PBE [a]	HF	G_0W_0 [b]	OEP-RPA [c]	GKS-spRPA
MAE	3.83	0.65	0.64	0.26	0.30
MSE	3.83	−0.31	0.64	−0.08	−0.29
Max AE	6.49	2.22	1.29	0.84	0.68

[a] Ref. [72]
[b] Ref. [72]
[c] Ref. [16]

For ionization potentials of neutral molecules in the GW27 benchmark [27, 72], OEP-RPA and GKS-spRPA reduce the errors by ∼50% compared to the G_0W_0 method, see Table II. Both OEP-RPA and GKS-spRPA have similar mean absolute errors of ∼0.3 eV for the GW27 testset. The mean signed errors show that GKS-spRPA ionization potentials are systematically too large, whereas the OEP-RPA HOMO energies can be too small or too large, as is also reflected in higher maximum absolute deviations.

OEP-RPA and GKS-spRPA quasiparticle energies differ substantially for HOMO-LUMO gaps, see Table III: OEP-RPA HOMO-LUMO gaps do not contain derivative discontinuities since they come from a local KS potential [75], and substantially underestimate fundamental gaps. G_0W_0 and GKS-spRPA, on the other hand, yield fundamental gaps within 1 eV of the coupled cluster reference results for unpolar molecules. For the highly polar tetracyanoethylene molecule, G_0W_0 and GKS-spRPA underestimate the fundamental gap by 3.3 and 1.7 eV, respectively, which may indicate residual self-interaction error.

TABLE III. Gaps (in eV) obtained as differences between the lowest unoccupied and highest occupied molecular orbital energies, and reference fundamental gaps computed using differences of CCSD(T) total energies (see SM for molecular structure details [59]). CCSD(T), GKS-spRPA and G_0W_0 calculations use aug-cc-pVTZ basis-sets while OEP-RPA results [16] were obtained using aug-cc-pCVTZ basis-sets [74]. For GKS-spRPA, the exchange-correlation potential is approximated using the PBE functional.

	OEP-RPA[a]	G_0W_0	GKS-spRPA	CCSD(T)
Li_2	1.23	4.43	5.28	4.76
Na_2	1.18	4.35	4.98	4.48
LiH	2.94	6.92	7.66	7.67
CH_3NO_2		9.82	11.48	11.41
$C_2(CN)_4$		6.96	8.48	10.29

[a] Ref. [16]

B. Noncovalent Interactions

GKS-spRPA substantially reduces the underbinding error observed in SL-RPA calculations of weakly interacting noble gas dimers and the dimers of S22 dataset [76], see Figs. S1 and S2.

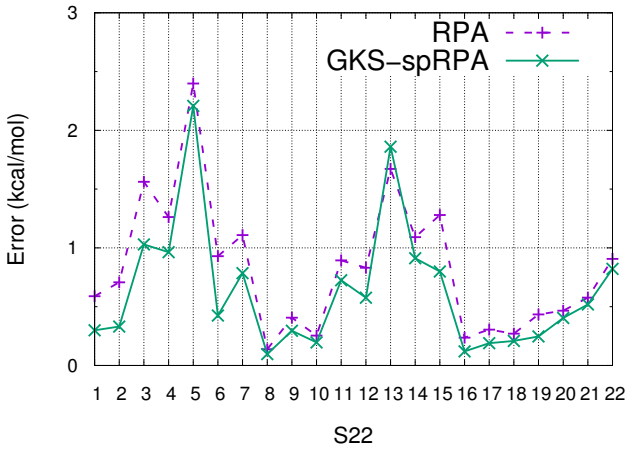

FIG. 1. Errors (computed−reference [77]) in binding energies for the dimers of S22 dataset. The PBE XC potential and aug-cc-pwCV(T,Q)Z[78] basis set extrapolation were used.

While RPA based on PBE [44] orbitals (RPA-PBE) produces hardly any binding for He_2 and substantially underbinds Ne_2, the nuclear potential energy curves obtained from GKS-spRPA closely resemble those obtained from the coupled cluster singles doubles with perturbative triples (CCSD(T)) [85] method, which is nearly exact for these systems.

Perturbative expansion of the GKS-spRPA energy around the SL ground state provides a rationale for the significant accuracy gains upon variational optimization for weak intermolecular interactions: The lowest-order

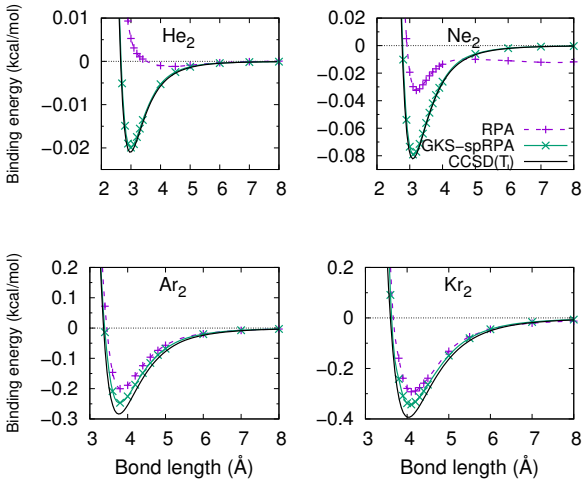

FIG. 2. Computed PECs of noble gas dimers compared to reference data [79–82]. aug-cc-pV6Z[83] basis sets were used for He_2, Ne_2 and Ar_2, and aug-cc-pV5Z[66, 84] basis sets were used for Kr_2; an additional set of atomic basis mid-bond functions was employed to speed up basis set convergence. The PBE XC potential was used.

total energy change in $\|H_0^{\mathrm{spRPA}} - H_0^{\mathrm{SL}}\|$ is

$$E^{(2)} = \sum_{ij\lambda\lambda'} (n_\lambda - n_{\lambda'}) \frac{|\langle \phi_{i\lambda}^{\mathrm{SL}} | H_0^{\mathrm{spRPA}} - H_0^{\mathrm{SL}} | \phi_{j\lambda'}^{\mathrm{SL}} \rangle|^2}{\epsilon_{i\lambda}^{\mathrm{SL}} - \epsilon_{j\lambda'}^{\mathrm{SL}}}. \quad (52)$$

The exchange portion of $H_0^{\mathrm{spRPA}} - H_0^{\mathrm{SL}}$ gives rise to the "single excitations" correction to SL-RPA, which were shown to be important for noncovalent bonding by Ren and co-workers [86]. Replacing the SL orbitals and orbital energies in Eq. (52) with the GKS-spRPA ones obtained in the first iteration corresponds to the "renormalized single excitations" (rSE) correction [32] plus additional correlation-relaxation contributions. While the rSE approach also improves considerably upon SL-RPA for noble-gas dimers, it spuriously overbinds in cases such as Ne_2 [32], whereas GKS-spRPA remains accurate, reflecting the additional stability resulting from variational optimization. Similar to orbital optimized RPA [19], GKS-spRPA thus implicitly accounts for singles corrections to all orders. A comparison of equilibrium properties for Ar_2 and Kr_2 and mean average errors for binding energies of S22 dataset shows that the GKS-spRPA improves upon both SL-RPA and OEP-RPA, see Table. IV.

C. Covalent Bonding

Compared to SL-RPA, GKS-spRPA reduces errors in atomization energies marginally but systematically for nearly all molecules contained in the G21 [88] and HEAT [89] atomization energy benchmarks. The mean absolute errors of SL-RPA and GKS-spRPA for binding energies of covalently bound molecules are within ~ 0.1 kcal/mol of

TABLE IV. Comparison of SL-RPA, OEP-RPA and GKS-spRPA results for molecular equilibriumproperties (bond lengths, r_e, in Å and binding energies, D_e, in kcal/mol), as well as mean absolute errors (MAEs) in binding energies of dimers in the S22 benchmark [76]. For SL-RPA and GKS-spRPA, the exchange-correlation potential was approximated using the PBE functional. Negative binding energies indicate bound states.

	Reference			
	SL	OEP [a]	GKS sp	Expt.
Ar_2				
r_e (Å)	3.84	3.85	3.79	3.775 [81]
D_e (kcal/mol)	−0.201	−0.193	−0.247	−0.284 [81]
Kr_2				
r_e (Å)	4.12	4.13	4.07	4.06 [82]
D_e (kcal/mol)	−0.293	−0.299	−0.343	−0.393 [82]
Be_2				
r_e (Å)	2.40	2.52	2.45	2.45 [87]
D_e (kcal/mol)	−1.018	+0.498	−1.911	−2.67 [87]
S22				
MAE (kcal/mol)	0.83	1.08	0.64	

[a] Refs. [15, 16]

TABLE V. Mean absolute (MAE), mean signed (MSE, computed−reference), and maximum absolute (Max AE) errors in kcal/mol for SL-RPA and GKS-spRPA using the G21 AE [88] and HEAT [89] atomization energy benchmarks. RPA and GKS-spRPA correlation energies were obtained using cc-pV(Q-5)Z[66] extrapolation for the G21 AE set, and using aug-cc-pV(Q-5)Z[66, 84] extrapolation for HEAT. Core orbitals with energies below −3 Hartree were frozen, and the exchange-correlation potential was approximated using the PBE functional.

Benchmark	Error Measure	RPA	GKS-spRPA
G21 AE	MAE	9.08	8.92
	MSE	−9.08	−8.84
	Max AE	25.39	25.43
HEAT	MAE	10.09	10.01
	MSE	−10.09	−10.01
	Max AE	25.81	24.77

each other, see Table V and SM [59]. This result reflects the accuracy of SL orbitals for covalent bonds. Orbital optimization using OEP-RPA, on the other hand, tends to worsen errors in reaction energies [16].

D. Beryllium Dimer

The potential energy curve (PEC) of beryllium dimer is a stringent test for approximate electron correlation theories, because it requires an accurate description of long-range dispersion interactions and strong near-degeneracy correlation between low-lying excited ^1P states of the isolated Be atoms [90]. The HF PEC is repulsive, second-order Møller-Plesset perturbation (MP2) theory produces binding energies nearly 3 times too small compared to experiment, while those from local and SL density functional theory are 3-5 times too large [91, 92]. Some of the SL functionals also display a small unphysical maximum. RPA-PBE produces too shallow well depth and an unphysical repulsive barrier at intermediate bonding distances, see Fig. 3, which neither the perturbative rSE correction nor second order screened exchange (SOSEX) correct entirely [4, 93, 94]. However, the combination of these corrections, i.e. RPA-PBE+rSE+SOSEX, removes this unphysical barrier [4]. OEP-RPA does not remove the barrier and produces a positive well-depth, i.e., Be_2 is unbound within OEP-RPA, see Fig. 3 and Table IV. GKS-spRPA not only removes the unphysical barrier, but also considerably improves the well-depth, yielding results close to the CCSD(T) ones. As CCSD(T) calculations are approximately 2 orders of magnitude more costly than GKS-spRPA calculations for many applications, this is a significant result, even though both methods fall short of capturing the strong static correlation at short bond distances.

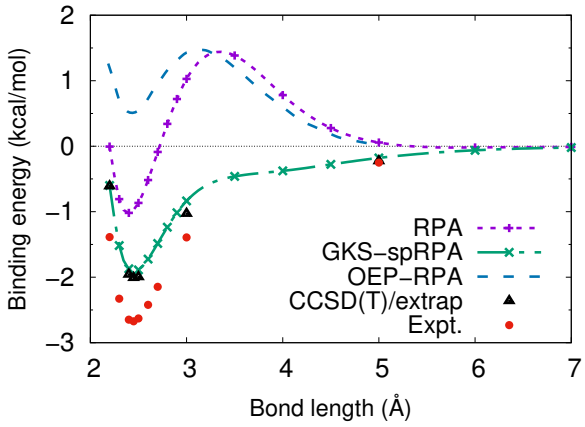

FIG. 3. Computed GKS-spRPA aug-cc-pwCV5Z [95] PECs of Be_2 molecule compared to OEP-RPA (using plane-wave basis sets with 50 Ry cutoff) [15], experiment [87] and complete basis-set limit CCSD(T) [96].

E. Stability of the GKS-spRPA Solution

The Coulson–Fischer point [97] (CFP) denotes the critical internuclear separation of a diatomic molecule where an approximate SCF solution spuriously breaks spin symmetry. The position of the CFP for a given method is an important measure of its ability to describe static correlation. For H_2, for example, the CFP occurs at $\sim$ 1.64 times the bond distance for HF, and $\sim$ 2.14 times the bond-length for most SL DFAs [98], which reflects the increased robustness of SL DFAs for small-gap sys-

tems such as transition metal compounds. The SL-RPA method using PBE orbitals inherits the instability from the PBE reference and displays spin symmetry breaking at the same internuclear distance, see Fig. 4. However, the energy of the spin-symmetry broken solution is *higher* than the one of the spin-restricted solution between 3 and 3.8 Bohr, and crosses the spin-restricted curve at a second CFP at 3.8 Bohr. This highly unphysical behavior reflects the lack of orbital stationarity of SL-RPA. GKS-spRPA, on the other hand, produces only one CFP at an internuclear distance of 3.8 Bohr which is ~ 2.71 times the bond-length. Our current results show no visually discernible first-order derivative discontinuity in the GKS-spRPA PEC at the CFP (see also Sec. III of the SM [59]), which is an undesirable feature of unregularized orbital-optimized MP2 theory [99]; however, a more detailed investigation is necessary to determine the analytical behavior of the two solutions at the CFP with certainty. While specialized density functionals for strong correlation without any instabilities have been devised [100], the present result underlines that GKS-spRPA yields a significant stability gain compared to existing SL functionals without sacrificing RPA's broad appeal for diverse molecular and condensed matter applications. Further improvement may require energy functionals beyond RPA.

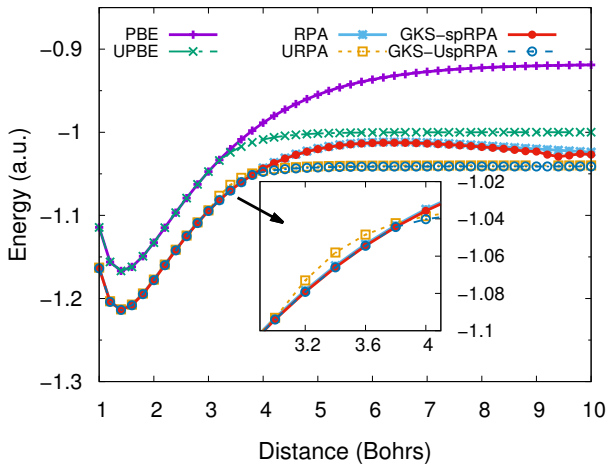

FIG. 4. PECs of H_2 using unrestricted and restricted PBE, RPA-PBE, and GKS-spRPA approaches. aug-cc-pV5Z [66] basis set and PBE potential were used.

Despite the good local stability properties of GKS-spRPA solutions, it is unclear whether the spRPA energy functional is globally well-defined. In rare cases, the unoccupied eigenvalues of the semicanonical Hamiltonian drop below the occupied ones, and the RPA correlation energy may become ill-defined. In such cases, the spRPA energy may not have a minimum as a functional of D. Indeed, in the GFT framework, the RPA energy as a functional of G_0 generated by nonlocal potentials is unbounded from below [101]. While this undesirable behavior can be mitigated to some extent by level shifting techniques familiar from OSC perturbation theory[102], it may be necessary to go consider fully FSC schemes beyond the present sp approximation to further improve the stability of RPA.

V. CONCLUSIONS

OSC optimization of approximate XC energy functionals with an explicit dependence on the KS potential requires specification of the KS potential as functional of the density and/or the KS orbitals and occupation numbers. However, most choices, including the so-called "exact" KS potential, produce an inconsistency between the KS potential and the functional derivative of the thus defined energy expression. Equivalently, the KS density used to evaluate the energy functional differs from the presumably more accurate Hellmann-Feynman density. This paradox appears to have been overlooked previously, and casts doubt onto OSC schemes for explicitly potential-dependent functionals such as OEP-RPA and OEP-based many-body perturbation theory.

This paradox is resolved by imposing the exact constraint on the KS potential that it must stationarize a given approximate XC energy functional at fixed KS orbitals and occupation numbers. If this condition uniquely determines the KS potential, this FSC potential is optimal in the sense that it is consistent with the energy functional it defines, and the resulting KS density equals the Hellmann-Feynman density. The FSC condition is a constraint on the KS potential and as such distinct from the OSC variational principle or OEP methods. If this condition gives rise to a unique KS potential, it provides a more consistent definition of the mapping between the KS potential and the best available approximation to the interacting density than the "exact" KS potential.

The GKS-spRPA scheme implements the FSC condition approximately, by requiring the GKS potentials defining the energy and obtained from its functional derivative to have the same ground state density matrix (and, equivalently, GKS determinant). Our results show that GKS-spRPA overcomes major limitations of SL DFAs and SL-RPA resulting from density-driven error: Negative ions are bound when they should be, and noncovalent interaction energies are significantly improved. GKS-spRPA covalent binding energies are only slightly more accurate than the SL-RPA ones, but the improvement is very systematic, as expected for a well-defined OSC variational approach. Errors previously attributed to missing beyond-RPA correlation, such as the spurious maximum in the Be PEC [4, 94] or inaccurate energy differences [52] vanish upon GKS optimization, suggesting that they may be primarily caused by lacking variational stability and functional selfconsistency rather than inherent errors of the RPA method.

The GKS-spRPA orbital energies match experimental ionization potentials and electron affinities of atoms and

molecules within a few tenths of an eV, surpassing the popular G_0W_0 method in accuracy. Analysis of the nonlocal GKS-spRPA correlation potential supports these observations, showing that quasiparticle *GW* energies are a first-order perturbative limit of canonical GKS-spRPA orbital energies. Unlike KS band gaps, the GKS-spRPA band gaps contain the energy derivative discontinuity at integer particle numbers, and thus accurately approximate the observable fundamental gap; this is of particular interest for infinite systems such as periodic solids, where IPs cannot be obtained from total energy differences.

The GKS-spRPA GKS solution is considerably more resilient to symmetry breaking than OSC SL KS solutions, as suggested by the location of the Coulson–Fischer point for the H_2 ground state. Moreover, GKS-spRPA eliminates the spurious second Coulson–Fischer point observed in non-OSC SL-RPA approaches. In conjunction with the above results, these improved stability characteristics provide additional evidence for the viability and robustness of the GKS-spRPA energy functional. In particular, the high stability of the GKS-spRPA solution bodes well for applications to response properties, whose accuracy can sensitively depend on the stability of the reference state.

From a computational viewpoint, the cost of a GKS-spRPA is on the order of that of a SL-RPA calculation times the number of GKS iterations; thus, GKS-spRPA calculations for systems with hundreds of atoms are within reach. KS-spRPA is considerably less costly than OEP-RPA, because it does not require ad-hoc regularization or special basis sets, and it is relatively straightforward to implement starting from RPA analytical gradients. While GKS-spRPA does not achieve complete functional selfconsistency, its considerably improved performance for energy differences and density-related properties compared to both SL RPA and OEP-RPA suggests that semicanonical projection provides a simple yet relatively accurate approximation to the FSC RPA potential.

The GKS scheme with semicanonical projection presented here may be applied beyond RPA to turn any conserving [103–105] energy functional of the KS one-particle Green's function into a density functional, and provides a solution to the conundrum of how to obtain accurate energy differences and choose the non-interacting system, e.g., in *GW* theory [106]: *All* observables, such as self-energies or response properties, are obtained as derivatives of a single, variationally stable energy functional of the KS density matrix, combining and enhancing the accuracy of RPA for energetics with the one of *GW* for quasiparticle spectra. Thus, GKS-spRPA is a step towards accurate, efficient, and universal electronic structure methods sharing favorable characteristics of both DFT and GFT.

ACKNOWLEDGMENTS

Discussions with Kieron Burke and Georg Kresse are acknowledged. This material is based upon work supported by the National Science Foundation under CHE-1464828 and CHE-1800431.

Appendix A: Functional Derivatives for Degenerate KS Density Matrices

The spRPA energy functional depends implicitly on the KS density matrix through the occupation numbers n_λ and the spectral projectors P_λ. However, the computation of functional derivatives with respect to D using the chain rule is not straightforward, because the P_λ are invariant under unitary transformations of orbitals with degenerate occupation numbers; as a result, the partial derivatives $\delta D/\delta P_\lambda$ can become singular, causing unphysical singularities in the functional derivative for degenerate D. Since noninteracting Fermion density matrices at zero temperature are usually highly degenerate, the possibility of degeneracy must be explicitly accounted for.

According to Eq. (19), D is a direct sum of degenerate blocks

$$\mathrm{n}_{\lambda\lambda'} = \delta_{\lambda\lambda'}\mathrm{n}_\lambda, \tag{A1}$$

where n_λ are $d_\lambda \times d_\lambda$ Hermitian matrices [55], and d_λ is the eigenvalue multiplicity. For a given D, the n_λ are multiples of the $d_\lambda \times d_\lambda$ identity, i.e., $\mathrm{n}_\lambda = n_\lambda 1$, where n_λ is a d_λ-fold degenerate occupation number. However, certain variations of D associated with changes in electron numbers can lift the degeneracy. To account for such variations, we do not require n_λ to be diagonal or degenerate in general.

The remaining degrees of freedom correspond to unitary transformations between orbitals with different occupation numbers. A convenient orbital parameterization is

$$|\phi_{i\lambda}(\kappa)\rangle = e^{\kappa}\,|\phi_{i\lambda}\rangle\,, \tag{A2}$$

where

$$\kappa = \sum_{\lambda\lambda'} \kappa_{\lambda\lambda'}, \tag{A3}$$

and unitarity implies that the $d_\lambda \times d_{\lambda'}$ blocks $\kappa_{\lambda\lambda'}$ satisfy

$$\kappa^\dagger_{\lambda\lambda'} = -\kappa_{\lambda'\lambda}. \tag{A4}$$

As a result, $\kappa_{\lambda\lambda} = 0$, i.e., transformations between degenerate orbitals are excluded. The spectral projectors

$$\mathrm{P}_\lambda = \sum_{i,j=1} |\phi_{i\lambda}\rangle\,\langle\phi_{j\lambda}| \tag{A5}$$

transform as

$$\mathrm{P}_\lambda(\kappa) = e^{\kappa}\mathrm{P}_\lambda e^{-\kappa}. \tag{A6}$$

The total number of independent variables contained in n and κ equals that of D.

Consider a variation of D around a given $\mathrm{D}^{(0)}$ corresponding to $\mathrm{n}_\lambda = \mathrm{n}_\lambda^{(0)} = n_\lambda 1$, $\kappa = 0$. The rank four partial derivative tensor

$$\left.\frac{\partial \mathrm{D}_{\lambda i \lambda' j}}{\partial \mathrm{n}_{\mu k l}}\right|_{\mathrm{D}^{(0)}} = \delta_{\lambda\lambda'}\delta_{\lambda\mu}\delta_{ik}\delta_{jl} \tag{A7}$$

is invertible for each $\lambda = \lambda' = \mu$ diagonal block. Similarly,

$$\left.\frac{\partial \mathrm{D}_{\lambda i \lambda' j}}{\partial \kappa_{\mu k \mu' l}}\right|_{\mathrm{D}^{(0)}} = \delta_{\lambda\mu}\delta_{\lambda'\mu'}\delta_{ik}\delta_{jl}(n_{\lambda'} - n_\lambda), \quad \lambda \neq \lambda' \tag{A8}$$

is invertible for each $\lambda' \neq \lambda$, because $n_{\lambda'} - n_\lambda \neq 0$ by construction. Adopting a short-hand matrix notation which implies the subindices of each λ block, Eq. (A7) may be written

$$\left.\frac{\partial \mathrm{D}_{\lambda\lambda'}}{\partial \mathrm{n}_\mu}\right|_{\mathrm{D}^{(0)}} = 1_{\lambda\mu} \otimes 1_{\mu\lambda'}, \tag{A9}$$

and Eq. (A8) becomes

$$\left.\frac{\partial \mathrm{D}_{\lambda\lambda'}}{\partial \kappa_{\mu\mu'}}\right|_{\mathrm{D}^{(0)}} = (n_{\lambda'} - n_\lambda)\, 1_{\lambda\mu} \otimes 1_{\mu'\lambda'}, \quad \lambda \neq \lambda'. \tag{A10}$$

The chain rule finally yields

$$\frac{\partial}{\partial \mathrm{D}_{\lambda\lambda'}} = \begin{cases} \frac{1}{n_{\lambda'} - n_\lambda}\frac{\partial}{\partial \kappa_{\lambda\lambda'}}, & \lambda \neq \lambda', \\ \frac{\partial}{\partial \mathrm{n}_\lambda}, & \lambda = \lambda', \end{cases} \tag{A11}$$

where the partial derivatives have been evaluated at $\mathrm{D} = \mathrm{D}^{(0)}$.

Appendix B: Density Matrix Derivative of the sp Green's Function

Eq. (26) expresses $\mathrm{G}_0(\omega)$ as an explicit functional of the occupation number matrices n_λ and the spectral projectors P_λ, as well as the sp Hamiltonian $\tilde{\mathrm{H}}_0$. Parameterizing the orbitals according to Eq. (A2) and using Eq. (A11), the partial density matrix derivative of $\mathrm{G}_0(\omega)$ for $\tilde{\mathrm{H}}_0$, evaluated at $\mathrm{D} = \mathrm{D}^{(0)}$, is straightforward,

$$\left(\frac{\partial \mathrm{G}_{0\mu\mu'}(\omega)}{\partial \mathrm{D}_{\lambda\lambda'}}\right)^{(1)} = \begin{cases} \frac{1_{\mu\lambda}\otimes \mathrm{G}_{0\lambda'\mu'}(\omega) - \mathrm{G}_{0\mu\lambda}(\omega)\otimes 1_{\lambda'\mu'}}{n_{\lambda'} - n_\lambda}, & \lambda \neq \lambda', \\ \pi i \left(1_{\mu\lambda} \otimes [\delta(\omega - \tilde{\mathrm{H}}_{0\lambda})]_{\lambda'\mu'} + 1_{\lambda'\mu'} \otimes [\delta(\omega - \tilde{\mathrm{H}}_{0\lambda})]_{\mu\lambda}\right), & \lambda = \lambda'. \end{cases} \tag{B1}$$

Here, the identity

$$\left.\frac{\partial [\mathrm{n}_\lambda^{1/2}]_{kl}}{\partial \mathrm{n}_{\lambda ij}}\right|_{\mathrm{n}_\lambda^{(0)}} = \frac{1}{2n_\lambda^{1/2}}\delta_{ik}\delta_{jl} \tag{B2}$$

was employed to evaluate the occupation number matrix derivatives.

Appendix C: Density Matrix Derivative Arising from Changes in $\tilde{\mathrm{H}}_0$

According to Eq. (20), the sp Hamiltonian depends on D through variations of the orbitals as well as through the SL Hamiltonian $\mathrm{H}_0^{\mathrm{SL}}[\mathrm{D}]$. Using the techniques of Sec. A, we obtain two partial derivatives of the sp Hamiltonian blocks at $\mathrm{D} = \mathrm{D}_0$,

$$\left(\frac{\partial \tilde{\mathrm{H}}_{0\mu\mu}[\mathrm{D}]}{\partial \mathrm{D}_{\lambda\lambda'}}\right)^{(2)} = \begin{cases} \frac{1_{\mu\lambda}\otimes \mathrm{H}^{\mathrm{SL}}_{0\lambda'\mu} - \mathrm{H}^{\mathrm{SL}}_{0\mu\lambda}\otimes 1_{\lambda'\mu}}{n_\lambda - n_{\lambda'}}, & \lambda \neq \lambda', \\ 0, & \lambda = \lambda', \end{cases} \tag{C1}$$

and

$$\left(\frac{\partial \tilde{\mathrm{H}}_{0\mu\mu}[\mathrm{D}]}{\partial \mathrm{D}_{\lambda\lambda'}}\right)^{(3)} = \frac{\partial \mathrm{H}^{\mathrm{SL}}_{0\mu\mu}[\mathrm{D}]}{\delta \mathrm{D}_{\lambda\lambda'}} = \mathrm{F}^{\mathrm{HXC}}_{\mu\mu\lambda\lambda'}. \tag{C2}$$

Here, $\mathrm{F}^{\mathrm{HXC}}$ denotes the rank-four tensor operator representing the SL Hartree-, exchange, and correlation kernel. In keeping with the main text, superscript (2) denotes for partial derivatives arising from the semicanonical projection, and superscript (3) denotes partial derivatives arising from changes of the SL Hamiltonian $\mathrm{H}_0^{\mathrm{SL}}[\mathrm{D}]$.

By Eq. (26), the total derivative of the sp Green's function with respect to the sp Hamiltonian is

$$\frac{\partial \mathrm{G}_{0\mu\mu'}(\omega)}{\partial \tilde{\mathrm{H}}_{0\lambda\lambda}} = \delta_{\mu\mu'}\Big(\mathrm{n}_\mu^{1/2}(\omega - \tilde{\mathrm{H}}_{0\lambda} - i0^+)^{-1}_{\mu\lambda} \otimes (\omega - \tilde{\mathrm{H}}_{0\lambda} - i0^+)^{-1}_{\lambda\mu'}\mathrm{n}_{\mu'}^{1/2} + (1 - \mathrm{n})_\mu^{1/2}(\omega - \tilde{\mathrm{H}}_{0\lambda} + i0^+)^{-1}_{\mu\lambda} \otimes (\omega - \tilde{\mathrm{H}}_{0\lambda} + i0^+)^{-1}_{\lambda\mu'}(1 - \mathrm{n})_{\mu'}^{1/2}\Big). \tag{C3}$$

Combining Eqs. (C1) - (C3) by the chain rule, the remaining partial derivatives of G_0 are

$$\left(\frac{\partial \mathrm{G}_{0\mu\mu'}}{\partial \mathrm{D}_{\lambda\lambda'}}\right)^{(2)} = \delta_{\mu\mu'} \begin{cases} (\omega - \tilde{\mathrm{H}}_0 - i0^+)^{-1}_{\mu\lambda} \otimes [\mathrm{H}_0^{\mathrm{SL}}(\omega - \tilde{\mathrm{H}}_0 - i0^+)^{-1}]_{\lambda'\mu'} \frac{n_\lambda}{n_\lambda - n_{\lambda'}} \\ \quad +(\omega - \tilde{\mathrm{H}}_0 + i0^+)^{-1}_{\mu\lambda} \otimes [\mathrm{H}_0^{\mathrm{SL}}(\omega - \tilde{\mathrm{H}}_0 + i0^+)^{-1}]_{\lambda'\mu'} \frac{1-n_\lambda}{n_\lambda - n_{\lambda'}} \\ \quad -[(\omega - \tilde{\mathrm{H}}_0 - i0^+)^{-1}\mathrm{H}_0^{\mathrm{SL}}]_{\mu\lambda} \otimes (\omega - \tilde{\mathrm{H}}_0 - i0^+)^{-1}_{\lambda'\mu'} \frac{n_{\lambda'}}{n_\lambda - n_{\lambda'}} \\ \quad +[(\omega - \tilde{\mathrm{H}}_0 + i0^+)^{-1}\mathrm{H}^{\mathrm{SL}}]_{\mu\lambda} \otimes (\omega - \tilde{\mathrm{H}}_0 + i0^+)^{-1}_{\lambda'\mu'} \frac{1-n_{\lambda'}}{n_\lambda - n_{\lambda'}}, & \lambda \neq \lambda', \\ 0, & \lambda = \lambda'. \end{cases} \tag{C4}$$

The HXC kernel part is

$$\left(\frac{\partial \mathrm{G}_{0k\mu l\mu'}}{\partial \mathrm{D}_{i\lambda j\lambda'}}\right)^{(3)} = \delta_{\mu\mu'} \Big[(\omega - \tilde{\mathrm{H}}_0 - i0^+)^{-1}\mathrm{F}^{\mathrm{HXC}}_{\lambda\lambda'}(\omega - \tilde{\mathrm{H}}_0 - i0^+)^{-1} n_\mu + (\omega - \tilde{\mathrm{H}}_0 + i0^+)^{-1}\mathrm{F}^{\mathrm{HXC}}_{\lambda\lambda'}(\omega - \tilde{\mathrm{H}}_{0\mu} + i0^+)^{-1}(1 - n_\mu)\Big]_{\mu\mu'}, \tag{C5}$$

where matrix multiplication is implied for the first two indices of $\mathrm{F}^{\mathrm{HXC}}$.

The chain rule also affords an explicit expression for the unrelaxed RPA difference density matrix,

$$\mathrm{T}_{\lambda\lambda'} = \delta_{\lambda\lambda'} \int_{-\infty}^{\infty} \frac{d\omega}{2\pi} \Big[(\omega - \tilde{\mathrm{H}}_0 - i0^+)^{-1}\Sigma^{\mathrm{C}}(\omega)(\omega - \tilde{\mathrm{H}}_0 - i0^+)^{-1} n_\lambda + (\omega - \tilde{\mathrm{H}}_0 + i0^+)^{-1}\Sigma^{\mathrm{C}}(\omega)(\omega - \tilde{\mathrm{H}}_0 + i0^+)^{-1}(1 - n_\lambda)\Big]_{\lambda\lambda'}, \tag{C6}$$

which follows from Eqs. (50), (40), and (C3).

[1] D. Pines and D. Bohm, Phys. Rev. **85**, 338 (1952).
[2] M. Gell-Mann and K. A. Brueckner, Phys. Rev. **106**, 364 (1957).
[3] H. Eshuis, J. E. Bates, and F. Furche, Theor. Chem. Acc. **131**, 1084 (2012).
[4] X. Ren, P. Rinke, C. Joas, and M. Scheffler, J. Mater. Sci. **47**, 7447 (2012).
[5] A. Heßelmann and A. Görling, Mol. Phys. **109**, 2473 (2011).
[6] J. F. Dobson and T. Gould, J. Phys. Condens. Matter **24**, 073201 (2012).
[7] S. Lebègue, J. Harl, T. Gould, J. G. Ángyán, G. Kresse, and J. F. Dobson, Phys. Rev. Lett. **105**, 196401 (2010).
[8] G. P. Chen, V. K. Voora, M. M. Agee, S. G. Balasubramani, and F. Furche, Annu. Rev. Phys. Chem. **68**, 421 (2017).
[9] F. Furche, Phys. Rev. B **64**, 195120 (2001).
[10] M.-C. Kim, E. Sim, and K. Burke, Phys. Rev. Lett. **111**, 073003 (2013).
[11] A. Wasserman, J. Nafziger, K. Jiang, M.-C. Kim, E. Sim, and K. Burke, Ann. Rev. Phys. Chem. **68**, 555 (2017).
[12] D. Lee, F. Furche, and K. Burke, J. Phys. Chem. Lett. **1**, 2124 (2010).
[13] A. J. Cohen, P. Mori-Sanchez, and W. Yang, Science **321**, 792 (2008).
[14] M. Hellgren, F. Caruso, D. R. Rohr, X. Ren, A. Rubio, M. Scheffler, and P. Rinke, Phys. Rev. B **91**, 165110 (2015).
[15] N. L. Nguyen, N. Colonna, and S. de Gironcoli, Phys. Rev. B **90**, 045138 (2014).
[16] P. Bleiziffer, A. Heßelmann, and A. Görling, J. Chem. Phys. **139**, 084113 (2013).
[17] P. Verma and R. J. Bartlett, J. Chem. Phys. **136**, 044105 (2012).
[18] M. Hellgren and U. von Barth, Phys. Rev. B **76**, 075107 (2007).
[19] Y. Jin, D. Zhang, Z. Chen, N. Q. Su, and W. Yang, J. Phys. Chem. Lett. **8**, 4746 (2017).
[20] R. W. Godby, M. Schlüter, and L. J. Sham, Phys. Rev. B **37**, 10159 (1988).
[21] M. S. Hybertsen and S. G. Louie, Phys. Rev. B **34**, 5390 (1986).
[22] G. Onida, L. Reining, and A. Rubio, Rev. Mod. Phys. **74**, 601 (2002).
[23] M. van Schilfgaarde, T. Kotani, and S. Faleev, Phys. Rev. Lett. **96**, 226402 (2006).
[24] F. Kaplan, M. E. Harding, C. Seiler, F. Weigend, F. Evers, and M. J. van Setten, J. Chem. Theory Comput. **12**, 2528 (2016).
[25] G. Borghi, A. Ferretti, N. L. Nguyen, I. Dabo, and N. Marzari, Phys. Rev. B **90**, 075135 (2014).
[26] S. Refaely-Abramson, S. Sharifzadeh, N. Govind, J. Autschbach, J. B. Neaton, R. Baer, and L. Kronik, Phys. Rev. Lett. **109**, 226405 (2012).
[27] M. J. van Setten, F. Weigend, and F. Evers, J. Chem. Theory Comput. **9**, 232 (2013).
[28] B. Holm and U. von Barth,

Phys. Rev. B **57**, 2108 (1998).
[29] A. Stan, N. E. Dahlen, and R. van Leeuwen, Europhys. Lett. **76**, 298 (2006).
[30] F. Caruso, P. Rinke, X. Ren, A. Rubio, and M. Scheffler, Phys. Rev. B **88**, 075105 (2013).
[31] A. Seidl, A. Görling, P. Vogl, J. A. Majewski, and M. Levy, Phys. Rev. B **53**, 3764 (1996).
[32] X. Ren, P. Rinke, G. E. Scuseria, and M. Scheffler, Phys. Rev. B **88**, 035120 (2013).
[33] J. E. Moussa, J. Chem. Phys. **140**, 014107 (2014).
[34] J. P. Perdew, W. Yang, K. Burke, Z. Yang, E. K. U. Gross, M. Scheffler, G. E. Scuseria, T. M. Henderson, I. Y. Zhang, A. Ruzsinszky, H. Peng, J. Sun, E. Trushin, and A. Görling, Proc. Natl. Acad. Sci. USA **114**, 2801 (2017).
[35] V. N. Staroverov, G. E. Scuseria, and E. R. Davidson, J. Chem. Phys. **124**, 141103 (2006).
[36] A. Heßelmann, A. W. Gotz, F. Della Sala, and A. Görling, J. Chem. Phys. **127**, 054102 (2007).
[37] T. Heaton-Burgess, F. A. Bulat, and W. Yang, Phys. Rev. Lett. **98**, 256401 (2007).
[38] T. Heaton-Burgess and W. Yang, J. Chem. Phys. **129**, 194102 (2008).
[39] A. Görling and M. Levy, Phys. Rev. A **50**, 196 (1994).
[40] A. Facco Bonetti, E. Engel, R. N. Schmid, and R. M. Dreizler, Phys. Rev. Lett. **86**, 2241 (2001).
[41] S. Ivanov, S. Hirata, I. Grabowski, and R. J. Bartlett, J. Chem. Phys. **118**, 461 (2003).
[42] W. Kohn and L. J. Sham, Phys. Rev. **140**, A1133 (1965).
[43] K. J. H. Giesbertz and E. J. Baerends, J. Chem. Phys. **132**, 194108 (2010).
[44] J. P. Perdew, K. Burke, and M. Ernzerhof, Phys. Rev. Lett. **77**, 3865 (1996).
[45] P. Hohenberg and W. Kohn, Phys. Rev. **136**, 864 (1964).
[46] P. R. T. Schipper, O. V. Gritsenko, and E. J. Baerends, Theor. Chem. Acc. **99**, 329 (1998).
[47] J. E. Harriman, Phys. Rev. A **34**, 29 (1986).
[48] R. Cuevas-Saavedra, P. W. Ayers, and V. N. Staroverov, J. Chem. Phys. **143**, 244116 (2015).
[49] E. H. Lieb, Int. J. Quant. Chem. **24**, 243.
[50] W. Yang, P. W. Ayers, and Q. Wu, Phys. Rev. Lett. **92**, 146404 (2004).
[51] J. Talman and W. Shadwick, Phys. Rev. A **14**, 36 (1976).
[52] P. Bleiziffer, M. Krug, and A. Görling, J. Chem. Phys. **142**, 244108 (2015).
[53] P. W. Ayers and W. Yang, J. Chem. Phys. **124**, 224108 (2006).
[54] F. Tandetzky, J. K. Dewhurst, S. Sharma, and E. K. U. Gross, Phys. Rev. B **92**, 115125 (2015).
[55] M. Levy and J. P. Perdew, "The constrained search formulation of density functional theory," in *Density Functional Methods In Physics*, edited by R. M. Dreizler and J. da Providência (Springer US, Boston, MA, 1985) pp. 11–30.
[56] D. C. Langreth and J. P. Perdew, Solid State Commun. **17**, 1425 (1975).
[57] O. Gunnarsson and B. I. Lundqvist, Phys. Rev. B **13**, 4274 (1976).
[58] J. Toulouse, W. Zhu, J. Ángyán, and A. Savin, Phys. Rev. A. **82**, 032502 (2010).
[59] See Supplemental Material at [URL will be inserted by publisher] for computational details, benchmark results, dependence on the XC potentials used, spin expectation values, and molecular structures.
[60] H. Eshuis, J. Yarkony, and F. Furche, J. Chem. Phys. **132**, 234114 (2010).
[61] T. Gilbert, Phys. Rev. B **12**, 2111 (1975).
[62] K. Pernal, Phys. Rev. Lett. **94**, 233002 (2005).
[63] F. Aryasetiawan and O. Gunnarsson, Rep. Prog. Phys. **61**, 237 (1998).
[64] B. Ramberger, T. Schäfer, and G. Kresse, Phys. Rev. Lett. **118**, 106403 (2017).
[65] A. M. Burow, J. E. Bates, F. Furche, and H. Eshuis, J. Chem. Theory Comput. **10**, 180 (2014).
[66] T. H. Dunning, J. Chem. Phys. **90**, 1007 (1989).
[67] K. A. Peterson and C. Puzzarini, Theor. Chem. Acc. **114**, 283 (2005).
[68] K. R. Lykke, K. K. Murray, and W. C. Lineberger, Phys. Rev. A **43**, 6104 (1991).
[69] G. Haeffler, D. Hanstorp, I. Kiyan, A. E. Klinkmüller, U. Ljungblad, and D. J. Pegg, Phys. Rev. A **53**, 4127 (1996).
[70] C. Blondel, C. Delsart, and F. Goldfarb, J. Phys. B **34**, L281 (2001).
[71] H. Hotop and W. C. Lineberger, J. Chem. Phys. **58**, 2379 (1973).
[72] K. Krause, M. E. Harding, and W. Klopper, Molecular Physics **113**, 1952 (2015).
[73] F. Weigend and R. Ahlrichs, Phys. Chem. Chem. Phys. **7**, 3297 (2005).
[74] D. E. Woon and T. H. Dunning, J. Chem. Phys. **103**, 4572 (1995).
[75] Y. M. Niquet and X. Gonze, Phys. Rev. B **70**, 245115 (2004).
[76] P. Jurecka, J. Sponer, J. Cerny, and P. Hobza, Phys. Chem. Chem. Phys. **8**, 1985 (2006).
[77] T. Takatani, E. G. Hohenstein, M. Malagoli, M. S. Marshall, and C. D. Sherrill, J. Phys. Chem. **132**, 144104 (2010).
[78] K. A. Peterson and T. H. Dunning Jr., J. Chem. Phys. **117**, 10548 (2002).
[79] T. van Mourik and T. H. D. Jr., J. Chem. Phys. **111**, 9248 (1999).
[80] R. Hellmann, E. Bich, and E. Vogel, Mol. Phys. **106**, 133 (2008).
[81] K. Patkowski, G. Murdachaew, C.-M. Fou, and K. Szalewicz, Mol. Phys. **103**, 2031 (2005).
[82] J. M. Waldrop, B. Song, K. Patkowski, and X. Wang, J. Chem. Phys. **142**, 204307 (2015).
[83] A. K. Wilson, T. van Mourik, and T. H. Dunning Jr., J. Mol. Struct. (THEOCHEM) **388**, 339 (1996).
[84] T. H. Dunning, K. A. Peterson, and A. K. Wilson, J. Chem. Phys. **114**, 9244 (2001).
[85] K. Raghavachari, G. W. Trucks, J. A. Pople, and M. Head-Gordon, Chem. Phys. Lett. **157**, 479 (1989).
[86] X. G. Ren, A. Tkatchenko, P. Rinke, and M. Scheffler, Phys. Rev. Lett. **106**, 153003 (2011).
[87] K. Patkowski, V. Špirko, and K. Szalewicz, Science **326**, 1382 (2009).
[88] D. Feller and K. A. Peterson, J. Chem. Phys. **110**, 8384 (1999).
[89] A. Tajti, P. G. Szalay, A. G. Császár, M. Kállay, J. Gauss, E. F. Valeev, B. A. Flowers, J. Vázquez, and J. F. Stanton, J. Chem. Phys. **121**, 11599 (2004).

[90] I. Røeggen and J. Almlöf, Int. J. Quantum Chem. **60**, 453 (1996).
[91] I. C. Gerber and J. G. Ángyán, Chem. Phys. Lett. **416**, 375 (2005).
[92] V. F. Lotrich, R. J. Bartlett, and I. Grabowski, Chem. Phys. Lett. **405**, 43 (2005).
[93] J. Paier, B. G. Janesko, T. M. Henderson, G. E. Scuseria, A. Grüneis, and G. Kresse, J. Chem. Phys. **132**, 094103 (2010).
[94] N. Colonna, M. Hellgren, and S. de Gironcoli, Phys. Rev. B **93**, 195108 (2016).
[95] B. P. Prascher, D. E. Woon, K. A. Peterson, T. H. Dunning, and A. K. Wilson, Theor. Chem. Acc. **128**, 69 (2011).
[96] S. Sharma, T. Yanai, G. H. Booth, C. J. Umrigar, and G. K.-L. Chan, J. Chem. Phys. **140**, 104112 (2014).
[97] C. A. Coulson and I. Fischer, Phil. Mag. **40**, 386 (1949).
[98] R. Bauernschmitt and R. Ahlrichs, J. Chem. Phys. **104**, 9052 (1996).
[99] S. M. Sharada, D. Stck, E. J. Sundstrom, A. T. Bell, and M. Head-Gordon, Mol. Phys. **113**, 1802 (2015).
[100] A. D. Becke, J. Chem. Phys. **138**, 074109 (2013).
[101] S. Ismail-Beigi, Phys. Rev. B **81**, 195126 (2010).
[102] J. Lee and M. Head-Gordon, J. Chem. Theory Comput. **14**, 5203 (2018).
[103] J. M. Luttinger and J. C. Ward, Phys. Rev. **118**, 1417 (1960).
[104] G. Baym and L. P. Kadanoff, Phys. Rev. **124**, 287 (1961).
[105] A. Klein, Phys. Rev. **121**, 950 (1961).
[106] N. E. Dahlen, R. van Leeuwen, and U. von Barth, Phys. Rev. A **73**, 012511 (2006).